Received: 29 June 2021 | Revised: 12 August 2021 | Accepted: 12 August 2021

DOI: 10.1002/pol.20210503

REVIEW

JOURNAL OF POLYMER SCIENCE WILEY

Molecular design strategies for high-performance organic electrochemical transistors

Peiyun Li | **Ting Lei**

Key Laboratory of Polymer Chemistry and Physics of Ministry of Education, School of Materials Science and Engineering, Peking University, Beijing, China

Correspondence
Ting Lei, Key Laboratory of Polymer Chemistry and Physics of Ministry of Education, School of Materials Science and Engineering, Peking University, Beijing 100871, China.
Email: tinglei@pku.edu.cn

Funding information
the National Natural Science Foundation of China, Grant/Award Number: 22075001; the Open Fund of the State Key Laboratory of Luminescent Materials and Devices (South China University of Technology), Grant/Award Number: 2021-skllmd-02

Abstract

Organic electrochemical transistors (OECTs) utilize ion flow from the electrolyte to modulate the electrical conductivity of the whole bulk organic semiconductor channel. With the characteristic of mixed ionic-electronic conducting in the entire volume, OECTs exhibit high transconductance and act as good transducers, particularly in bioelectronics. To gain high-performance OECTs, developing novel high-performance polymeric semiconductors is important. In this article, operation principles, performance evaluations, and polymerization methods are first discussed. We then analyze the molecular design strategies for high-performance OECT materials and highlight the characteristics and effects of backbone design and side chain engineering. Finally, we discuss some neglected and unsolved issues and provide an outlook for the OECTs research and development.

KEYWORDS

organic electrochemical transistors, molecular design strategy, backbone design, side chain engineering

1 | INTRODUCTION

Organic electrochemical transistor (OECT) is a type of transistor whose organic semiconducting layer contacts directly with an electrolyte.[1,2] Unlike the double layer charge generation mechanism in organic field effect transistors (OFETs), the ions in the electrolyte of OECTs can penetrate into the organic film driven by voltage (below 1 V), which changes the conductance of the film. Therefore, OECTs are regarded as ion-electron transducers, and the semiconductors used in OECTs are also referred to as organic mixed ionic/electronic conductors (OMIECs), including conjugated polymers, conjugated polyelectrolytes (CPE), and so on.[3] Because of the ion-electron transformation in the bulk of OMIECs, OECTs show high-signal amplification capacity, which makes them suitable for the detection of small signals. Besides, the liquid environment, softness of organic semiconductors, and solution processing method make OECTs ideal for biocompatible devices.[4] With the characteristics mentioned above, OECTs are widely studied in the field of chemical and biological sensors,[5–8] biological interfaces,[9,10] and artificial synapses.[11–14]

The first OECT is developed by Wrighton and co-workers in 1984 using polypyrrole (PPy) as the semiconducting layer.[2] In the later 30 years, poly(3,4-ethylenedioxythiophene) doped with poly(styrene sulfonate) (PEDOT:PSS) (Figure 5A) has become the most popular material in OECTs due to its high conductivity, hydrophilicity, and commercial availability. While the high performance of PEDOT:PSS-based OECTs have shown many attractive applications, PEDOT:PSS still presents several drawbacks, including its (i) complex system, impeding the understanding on polymer structure-device performance, (ii) large current at zero bias, leading to high power consumption for wearable electronics, (iii) high acidity which may affect living systems.[15] To overcome those shortcomings, plenty of researches have

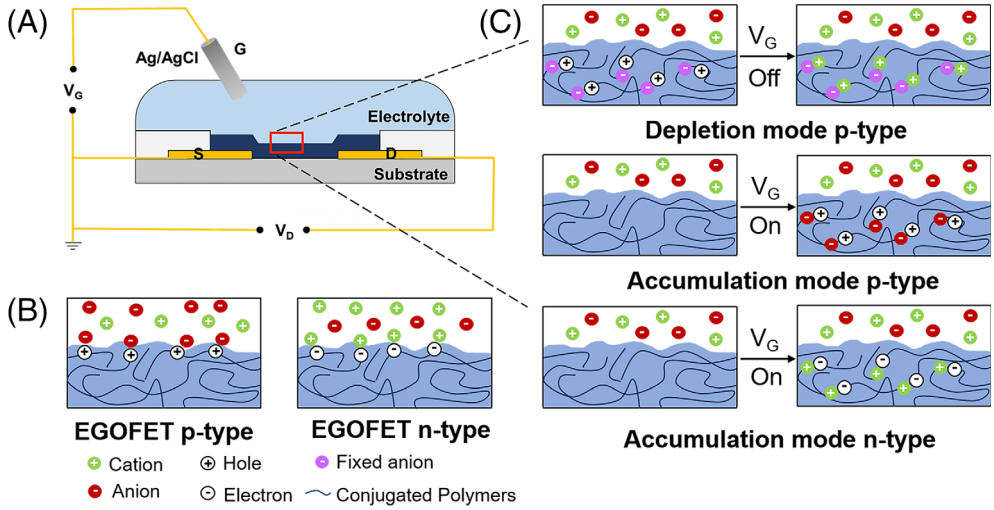

FIGURE 1 (A) Typical device structure of an OECT device. (B) Picture depicting the electrolyte/polymer interface of an EGOFET and having p-type (left) or n-type (right) polarity of operation. (C) Schematic illustration of the changes occurring in the electrolyte/polymer interface for OECTs working in depletion (top) and accumulation mode (middle for p-type and bottom for n-type). EGOFET, electrolyte-gated organic field effect transistor; OECT, organic electrochemical transistor

focused on modifying the PEDOT:PSS system,[16] while others concentrated on developing new polymer backbones. Their achievements greatly enriched the OECT materials family and many polymers have exhibited performances superior to PEDOT:PSS.

In this article, we aim to outline recent progress in the design of OMIECs and summarize the molecular design strategies for high-performance OECTs. In the first part, we focus on the electrolyte/polymer interface and the behavior of ions to introduce the operation principles, performance parameters, and benchmarks of an OECT device or material. In the second part, we review the main high-performance semiconductors and expound on the relationship between molecular structures and their OECT performances from two aspects: backbone design and side chain engineering. In this article, conjugated polymers for OECTs are labeled as the second-generation and third-generation semiconducting polymers according to Heeger's classification.[17] The second-generation semiconducting polymers mainly refer to the derivatives of polythiophene. The other polymers are classified as third-generation semiconducting polymers including donor–acceptor (D–A) polymers which are based on a combination of electron-rich (donor) and electron-deficient (acceptor) units, acceptor–acceptor polymers, and some ladder-type polymers. The main polymerization methods and small molecule structures of OECT materials are also introduced. In the last part, we give our overview on the challenges and future research directions in the development of OECTs.

2 | OPERATION PRINCIPLES, PERFORMANCE PARAMETERS, AND POLYMERIZATION OF OECTs

2.1 | Operation principles

In an OECT, the source (S) and drain (D) electrodes are connected by a semiconductor layer (channel), and the gate (G) can control the conductance of the film via an electrolyte (Figure 1A). When a bias voltage (V_D) is applied between the drain and source (grounded), charge carriers flow in the channel, producing current (I_D). The bias voltage (V_G) applied to the gate can drive ions in the electrolyte into the channel, change the conductance of the semiconductor and modulate I_D.

OECTs have a similar device structure to electrolyte-gated organic field effect transistors (EGOFETs). The major difference between OECTs and EGOFETs is that ions can/cannot penetrate into the polymer film (Figure 1B,C). For an EGOFET, its operation principle is similar to OFET, while the dielectric is an electrolyte. Ions in the electrolyte make directional migration driven by V_G, inducing an electrode double layer (EDL) on the electrolyte/semiconductor film interface. The induced carriers hugely change the film's conductivity and lead to the increment of I_D. For OECTs, there are two operational modes: depletion and accumulation mode. Some polymers work in the depletion mode, such as PEDOT:PSS. For OECTs work in the depletion mode, there are mobile carriers (holes) in pristine film, which makes the devices in on state at zero bias ($V_G = 0$ V). When a

negative V_G is applied, cations in the electrolyte penetrate into the film, inducing the disappearance of holes, and switch the devices into off state. For an OECT that works in the accumulation mode, the device is in off state at zero gate bias. When V_G drives anions (p-type) or cations (n-type) penetrate into the film, inducing holes or electrons, the device is switched from off state to on state.

Many researchers have studied and proven the existence of two operation principles (field-effect and electrochemical principles).[18–20] Ginger and co-workers utilized in situ electrochemical strain microscopy (ESM) and found that polymer semiconductors can simultaneously exhibit field-effect and electrochemical operation regimes, which are related to nanoscale film morphology, ion concentration, and electric potential.[21] The ion infiltration capacity of the polymer film, which is determined by the molecular structure and molecular packing, plays a key role in OECTs. Because of the presence of electrolytes, many design principles established over the past two decades for OFETs must be adjusted before applied to OECTs, and the role of hydrophilic side chains should be highlighted. In the second part of this article, some effective design principles for high-performance OECT semiconductors are introduced and summarized.

2.2 | Performance parameters

For OECTs, due to the high capacitor of the electrolyte, a small gate voltage ($|V_G| < 1$ V) can modulate channel current (I_D) via ion doping. The modulation relationship can be observed by transfer curves (I_D–V_G curve with a constant V_D bias) and output curves (I_D–V_D curve with a constant V_G bias). The steeper the transfer curve is, the larger the drain current change for a given gate voltage signal. According to the Bernards model,[22] the first derivative of the transfer characteristic, namely transconductance ($g_m = \partial I_D/\partial V_G$), can be fitted to the formula:

$$g_m = (W/L) \cdot d \cdot \mu \cdot C^* \cdot |(V_{th} - V_G)|, \quad (1)$$

where W, L, and d, are the channel width, length, and thickness, respectively, μ denotes the charge carrier mobility, C^* denotes the capacitance of the channel per unit volume, and V_{th} is the threshold voltage. We can also read out the on–off ratio ($I_{D,on}/I_{D,off}$) from the transfer curve, which is the symbol of transistors' switching performance.

g_m was considered as the figure of merit for OECTs and researchers sought after high g_m via many methods, including enhancing the Wd/L. Afterward, $g_{m,nom}$ ($g_m/[Wd/L]$) has been widely used as a comparison of different materials.[23] In recent years, Rivnay and coworkers labeled the product of mobility and volumetric charge storage capacity (μC^*) as the benchmark of OECT materials.[24] Huge C^* indicates superior ion penetration ability and high-charge storage properties. However, when ions infiltrate into semiconducting polymers, they can induce traps due to coulombic interactions and cause structural and energetic disorders, which will impede charge carrier transport and reducing μ.[25] Recently, the trade-off between μ and C^* has attracted more attention for the design of high-performance OECTs.[26]

Although Bernards model has been widely used, a few new models have recently been proposed to more accurately describe mixed ionic-electronic transport behavior in OECTs. Lüssem and coworkers took lateral ion currents in the channel into account and found that the equilibrium state of an OECT is not as the prediction of Bernards model.[27] They discovered that ion diffusion and accumulation have a large impact on the potential drop in the channel, which is a dynamic other than static process. In addition, some other models introduce more parameters to describe the OECT operation behavior.[28–30] These models further conform to the actual situation while they greatly increase the difficulty of comparison between channel materials and are seriously affected by the device configuration. Therefore, for a convenient and relatively fair comparison, μC^* obtained using the Bernards model has been widely used as a key parameter to compare the performance of different channel materials in this article.

For an OECT, one of the challenges is the long response time (including switching on (τ_{on}) and switching off time (τ_{off}), typically >100 μs), largely due to the slow migration rate of the ions. Therefore, the response speed is also an important parameter for OECTs. τ is determined both by electronic transit time (τ_e) and ion transit time (τ_i). The electronic transit time is described by $\tau_e = L^2/\mu V_d$, and τ_i is dictated by the product of the resistance of the electrolyte and the capacitance of the channel.[22,31] The kilohertz response speed of OECTs is adequate for quasi-static biosensor applications and some electrophysiological signals recording but limits their applications requiring fast response, such as electroencephalogram (EEG) measurement. The μC^* value and the other parameters of an OECT highly depend on the polymer chemical structures. Therefore, exploring molecular design strategies is necessary.

2.3 | Material type and synthesis

As we know, most OECT materials are polymers up to now. The crystallinity of polymer films is generally

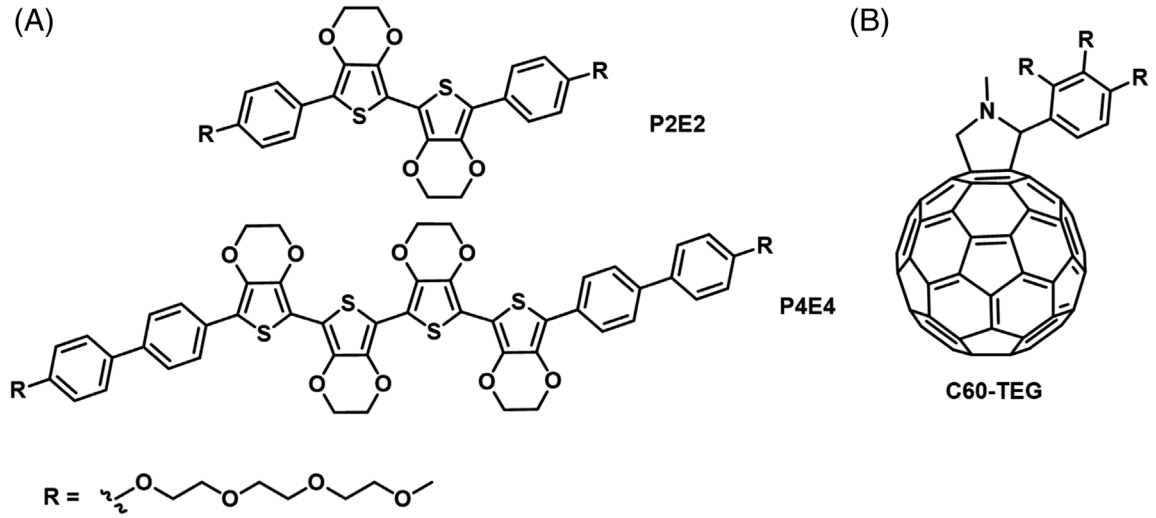

FIGURE 2 Chemical structures of two small-molecule OECT materials: (A) P2E2 and P4E4,[33] (B) C60-TEG.[34] OECT, organic electrochemical transistor

lower than that of small molecules. The amorphous morphology is of benefit to ion infiltration and maintenance of electron transport path in doped systems.[20,32] Compared with polymers, small molecules have higher purity and reproducibility. There are only two cases of small molecules OECTs up to now. Nielsen and coworkers built two p-type small molecules using the benzene and EDOT units, named P2E2 and P4E4[33] (Figure 2A). To improve charge injection and overcome the low viscosity of small molecule solutions, they blended these molecules with high-molecular weight polyethylene oxide (PEO). Although the performances of the small molecules are not outstanding (the highest μC^* value <1 F cm^{-1} V^{-1} s^{-1}), the design strategies and processing methods are enlightening. Ginger and coworkers designed a EG side chain grafted fullerene, named C60-TEG, as an n-type material for OECTs[34] (Figure 2B). The hydrophilic fullerene derivative shows a high-μC^* value of 7 ± 2 F cm^{-1} V^{-1} s^{-1}, which represents a promising prospect of small-molecule semiconductors for OECTs. There are few studies on small-molecule OECT materials so far, and the structure-performance relationship is not clear enough. Therefore, this article will focus on the molecular design of polymer OECTs in the next part.

The main polymerization methods for OECT polymers are shown in Figure 3. PEDOT:PSS (Figure 5A) and its derivatives are usually synthesized by oxidative polymerization or electropolymerization. Kumada catalyst polymerization is commonly used in polythiophene derivatives, such as poly(6[thiophene-3-yl]hexane-1-sulfonate) tetrabutylammonium (PTHS)[35] (Figure 3D). Stille polymerization is the most widely used method for OECT polymers, not only for polythiophene derivatives[23] but also for D–A polymers.[36] In general, a larger polymer molecular weight allows for better organic device performance. However, the molecular weight of D–A polymers is limited when grafted with EG side chain.[37,38] Recently, Lei et al. optimized the catalyst and solvent in Stille polymerization[39] and found that $Pd(PPh_3)_4$/$Pd(PPh_3)_2Cl_2$ and *N*,*N*-dimethylformamide/chlorobenzene 1:1 mixture can provide significantly higher molecular weights, which can solve the low-molecular weight issue for ethylene glycol (EG) side chain polymers.

The aforementioned polymerization methods usually have some disadvantages such as the use of hazardous monomers, toxic solvents, or transition metal catalysts.[40] For environmental protection and bioelectronic applications, several greener polymerization methods have been applied for OECTs, including aldol condensation polymerization for PgNaN[38] (Figure 7D), and direct arylation polymerization for ProDOT(OE)-DMP[41] (Figure 5A). It is believed that polymerization methods will continue expanding to fully release the potential of molecular structure design for high-performance OECTs.

3 | MOLECULAR DESIGN STRATEGIES FOR HIGH-PERFORMANCE OECTs

Different from OFET materials that only consider charge carrier mobility, both charge carrier (hole/

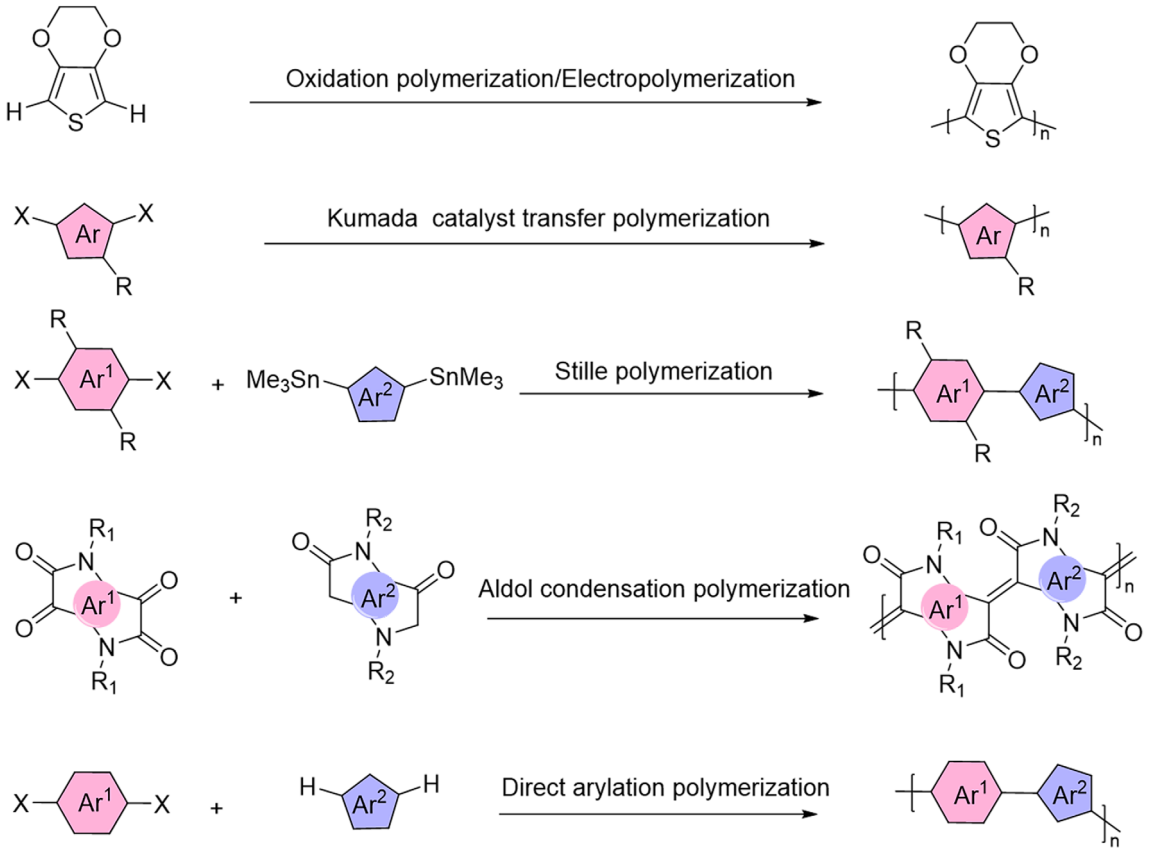

FIGURE 3 Polymerization methods used for OECT polymers. Ar stands for aromatic rings and R stands for side chains. OECT, organic electrochemical transistor

electron) transport and ion diffusion are important for a high-performance OECT material. Improving ion penetration capacity through side chain engineering for classic polythiophene system and investigating additives for PEDOT:PSS system is in full flourish. In addition, the polythiophene system has also been further expanded to regulate the material properties, adding fused rings in the backbone such as bithiophene, benzodithiophene, and so on. These strategies improved device performance to a large extent and become the basic rules for OECT molecular designing. However, modifications to the second-generation semiconducting polymers are limited, especially on the energy level. To further develop n-type materials and enhance performances of OECTs, D-A polymers with different backbones and side chains have been introduced in OECTs and have shown relatively excellent performance. In this part, we review the second and third-generation semiconducting polymers for OECT and describe their design strategies from backbone design and side chain engineering. Besides, their polymerization methods and small molecule structures for OECT materials are also introduced briefly.

3.1 | The second-generation semiconducting polymers for OECTs

3.1.1 | Side chain engineering

The second-generation semiconducting polymers for OECTs are based on polythiophene derivatives. They all exhibited p-type behaviors and their properties can be largely modulated by side chains engineering. For OFETs, alkyl side chains are usually used to enhance solubility and tune molecular packings. However, for OECTs, alkyl side chains are not preferred due to their hydrophobicity and poor ion infiltration capacity,[19] while EG side chains and ionic side chains are more widely used to ensure adequate hydrophily and ionic affinity. Besides, the side chain will also interact with the main chain, affecting the energy level of the molecule, packing mode, and other properties.

Poly(3-hexylthiophene) (P3HT) (Figure 4A) is one of the earliest studied organic semiconductors in OFET. However, because of the hydrophobic alkyl side chains, the ions infiltration ability of P3HT film is poor, which leads to unsatisfactory behavior for OECTs. Therefore, adjusting the side chain to get a better ion migration

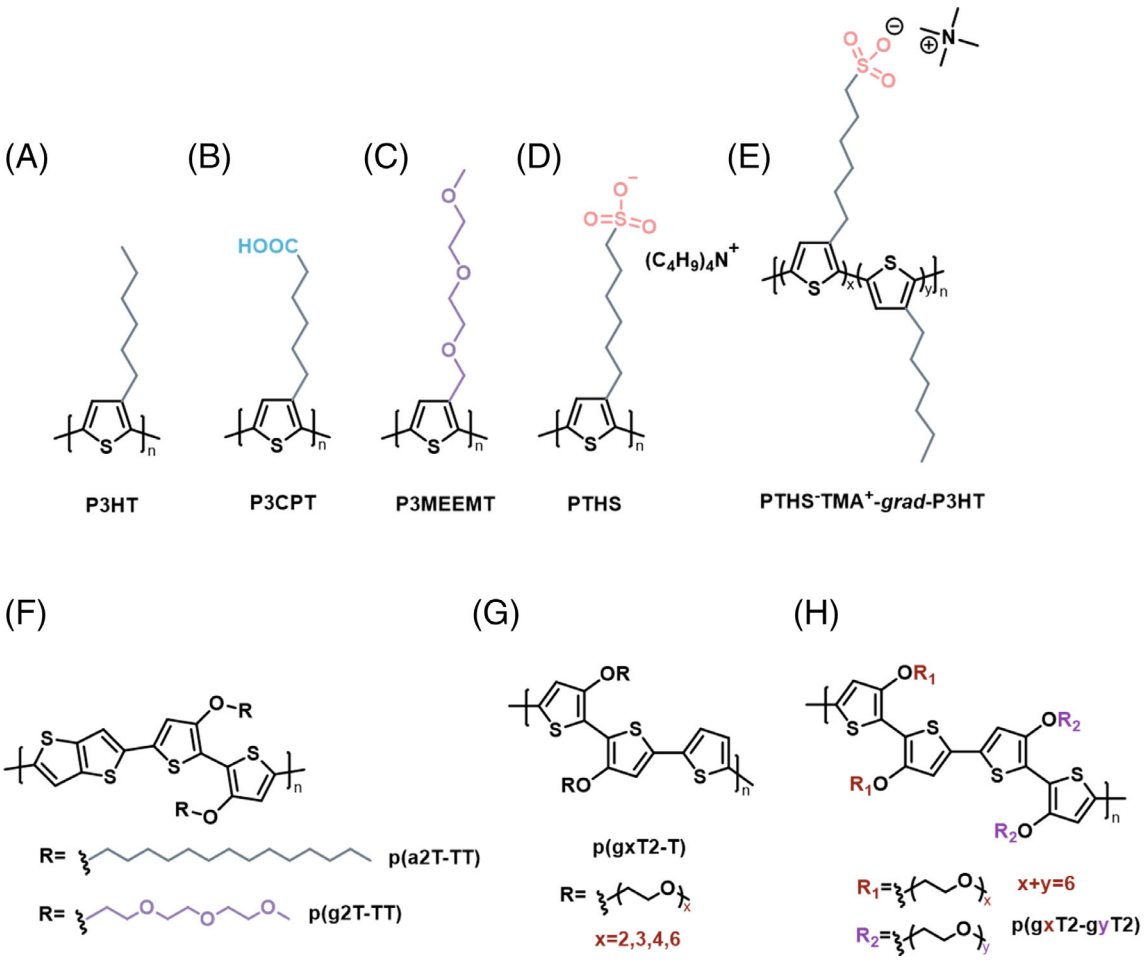

FIGURE 4 Chemical structures of the side chain engineering of second-generation semiconducting polymers for OECTs, (A) P3HT. (B) P3CPT.[18] (C) P3MEEMT.[20] (D) PTHS.[35] (E) $PTHS^-TMA^+$-grad-P3HT.[26] (F) p(g2T-TT) and p(g2T-TT).[19] (G) p(gxT2-T),[45] including g2T-T when x = 3. (H) p(gxT2-gyT2).[46] OECTs, organic electrochemical transistors

property is one of the main strategies to enhance the OECT performance of polythiophene derivatives.

P3MEEMT (Figure 4C) is a polythiophene derivative with EG-based side chains.[20] Compared to P3HT, P3MEEMT shows a faster ion injection speed, leading to better OECT performances. Furthermore, Ginger and co-workers found that hydration has a huge impact on both ion transport and carrier transport. On the one hand, larger hydrophobic anions can lower the threshold voltage, suggesting water may hinder the ions' infiltration. On the other hand, the presence of water may damage the electronic connectivity between the crystalline regions, thus lowering the charge carrier mobility in the solution. This work not only used side chain engineering to develop a new material but also revealed the important role of film morphology of OECTs. Afterward, Inal and Thelakkat et al. investigated the role of alkyl spacer on OECTs performance of P3MEEMT derivative and found that ethyl spacer effectively improved crystallinity and mixed-conduction properties.[42]

CPE are a class of conducting polymers possessing polar electrolyte groups covalently attached to the conjugated backbone.[43] The polar electrolyte groups make CPE hydrophilic and improve their ion mobility. Poly (3-carboxypentylthiophene) (P3CPT)[18] (Figure 4B), the end of the side chain of P3HT replaced by a carboxyl group, shows electrochemical operation mode under high gate voltage. Similarly, PTHS (Figure 4D)[35] leads to high-transconductance accumulation mode OECTs. Including EG as a co-solvent further improves transconductance and response time compared to devices from pristine PTHS films, demonstrating that film morphology also has a huge effect on carrier and ion transport for CPE.

However, the high solubility of $PTHS^-M^+$ (M^+ referred to different cations) polyelectrolytes may induce degradation during device operation, while the addition of a crosslinker to prevent degradation means a sacrifice of carrier and ion conductivity. It is an optional solution that adopting the strategy of copolymerization. Inal, Thelakkat, and co-workers developed a copolymer

PTHS$^-$TMA$^+$-co-P3HT (Figure 4E).[26] The copolymer is crystalline and easily oxidizable, thus enhancing the hole mobility (0.017 $cm^2\ V^{-1}\ s^{-1}$) and reducing the V_{th}. Moreover, high C^* (>100 F cm^{-3}) is achieved, indicating that the hydrophobic 3HT does not hamper ion transport. Besides, better stability in water is achieved by copolymerization, thus reducing the amount of cross-linker needed. Therefore, copolymerization, which combines hydrophilic segments (ionic side chain) and hydrophobic segments (alkyl side chain) is a promising strategy to obtain high-performance OECT materials.

Based on polythiophene, Rivnay and co-workers used p(a2T-TT) and p(g2T-TT) (Figure 4E) to control the operation mode through side chain engineering.[19] Both the alkyl and triethylene glycol (TEG) side chain are connected to the thiophene backbone by an oxygen atom because the intramolecular sulfur-oxygen interactions can induce backbone coplanarity and increase the effective conjugation length, which efficiently improves charge transport and decreases the ionization potential (IP). With alkyl side chains, p(a2T-TT) behaves in a mixed operation mode which means ions can penetrate into semiconductor film partially, deeper than EDL but shallower than the whole bulk. However, with the help of TEG side chains, p(g2T-TT) exhibits terrific OECT performance, including fast switching speed on the microsecond scale and high μC^* (261 F $cm^{-1}\ V^{-1}\ s^{-1}$). In the following research, Savva and co-workers confirmed that the increment of hydrophilic side chain content could lead to greater hydration and expansion of the channel during electrochemical doping.[44] Although the ion injection and transport are improved, the swelling negatively influences the electron transport and, consequently, the performance of OECTs. With the percentage of TEG side chains increasing from 0 (alkyl side chain) to 100% (p(g2T-TT)), g_m, μ, and C^* of devices are all improved, while a polymer with the same backbone and hexakis EG side chains exhibits lower g_m, μ, and C^* than p(g2T-TT), resulted from film deformation. Similar research was implemented by McCulloch and co-workers. The length of the EG side chain is optimized on g2T-T (Figure 4G).[45] The redistribution of side chain on different proportions is proved to strongly impact the water uptake, and p(g2T2-g4T2) realized the highest μC^* of 522 F $cm^{-1}\ V^{-1}\ s^{-1}$ and current retentions (Figure 4H).[46] Therefore, there is a trade-off between ionic and electronic conduction with the choice of proper EG side chains and content, which makes side chain engineering changeable but not random.

From the researches mentioned above, we can conclude that side chain engineering has a unique status in molecular design for OECTs. In backbone engineering that we will discuss below, EG side chains and ionic side chains are also used in the molecular structure and play an important role in ion transport.

3.1.2 | Backbone design

Backbone design based on the polythiophene system mainly focuses on introducing fused rings to modulate molecular planarity and stacking mode, thus improving charge transport. Here we will discuss benzodithiophene and alkylenedioxythiophene units used in OECTs.

Benzodithiophene is a conjugated building block with good planarity and linearity. Nielsen, Giovannitti, and co-workers designed a series of BDT (benzo[1,2-b:4,5-b′] dithiophene)-based polymers to elucidate structure–property guidelines required for accumulation mode OECTs[23,47] (Figure 5B). The alkoxy side chains in the 4,8-positions of BDT increase the electron density of the BDT structure due to the resonance effect. Thiophene (T), bithiophene (T2), thienothiophene (TT), TEG side chain functionalized bithiophene (g2T) and 3,3′-dimethoxy-2,2′-bithiophene (MeOT2) are comonomers that were chosen due to their electron-rich conjugated systems and high degrees of backbone coplanarity, thus achieving low operation voltages and good charge transport properties. These thiophenes comonomers bring in various charge distribution and degrees of backbone curvature, which influence energy level, side chain orientation, molecular packing, and consequently charge transport. Besides, g2T-T (Figure 4G) was designed to investigate the role of the π-conjugated backbone and its charge transport properties. gBDT-T, gBDT-T2, and gBDT-TT all have IPs around 4.7–4.9 eV, whereas the electron-rich gBDT-MeOT2, g2T-T, and the fully TEGylated gBDT-g2T have significantly lower IPs around 4.3–4.4 eV. g2T-T exhibits the best OECT performance due to its terrific carrier and ion transport. Polymers containing the TEGylated bithiophene unit (g2T-T and gBDT-g2T) are more electrochemically stable than polymers with the TEGylated benzodithiophene unit (gBDT-T, gBDT-T2) during cyclic voltammetry cycle and spectroelectrochemistry test. The reason initially was attributed to the lower IP and proper electrochemical potential window of g2T.[23] Afterward, through the analysis of infrared spectroscopy and density functional theory, it was thought that the actual cause might be the TEGylated BDT unit (gBDT-T2 and gBDT-TT) can potentially be oxidized at the 4,8-positions to form a quinone structure, which would result in a decrease of the donor strength as well as breaking the effective conjugation by the introduction of electron-withdraw quinone groups. However, gBDG-MeOT2 would not form a quinone structure mainly because the MeOT2 unit can stabilize

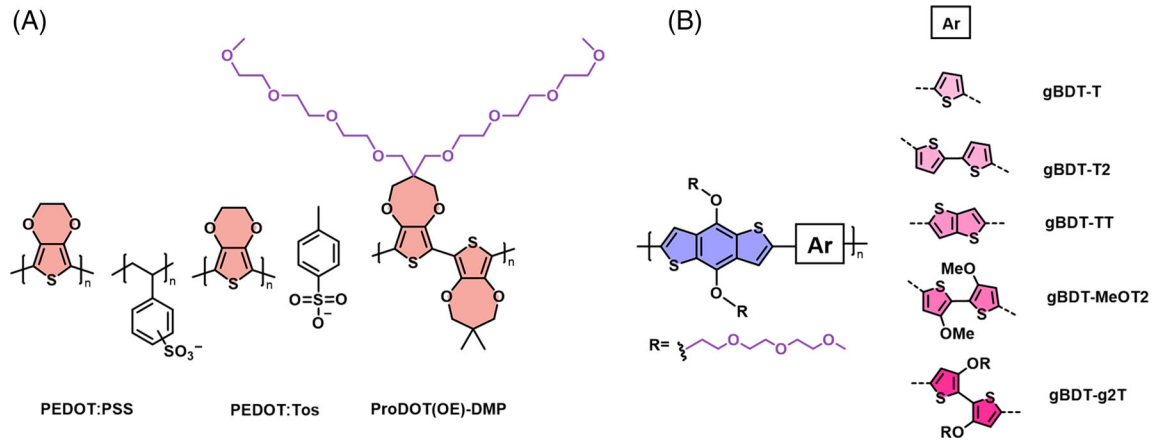

FIGURE 5 Chemical structures of the backbone design of second-generation semiconducting polymers for OECTs. (A) XDOT-based polymers, including PEDOT:PSS,[48] PEDOT:TOS[31] and ProDOT(OE)-DMP.[41] (B) BDT-based polymers.[23,47] BDT, benzo[1,2-b:4,5-b′] dithiophene; DMP, 2,2-dimethyl; OECTs, organic electrochemical transistors; PEDOT:PSS, poly(3,4-ethylenedioxythiophene) doped with poly(styrene sulfonate); PEDOT:Tos, poly(3,4-ethylenedioxythiophene) doped with tosylate; XDOT, 3,4-alkylenedioxythiophene

polarons on the polymer backbone due to the increased charge stabilization as well as a reduced orbital and charge density on the BDT groups.[47] The achievements inspire us that oligo(ether) chains directly link onto the electroactive backbone may render the polymer unstable and suffer irreversible degradation during electrochemical doping, while proper electron-rich donor units can effectively solve this problem.

For redox applications, 3,4-alkylenedioxythiophene (XDOT)-based polymers have several distinct advantages over general thiophene derivatives. Owing to the disubstitution of π-donating oxygen atoms, they are much easier to be oxidized. Furthermore, as the alkyl bridge can protect the conjugated backbone against nucleophilic attack, the polymers can exhibit high-redox stability.[41] These advantages make XDOT-based polymers promising materials for OECT.

PEDOT:PSS is the most widely used polymer for OECT. Poly(styrene sulfonate) is added as a dopant to induce holes in poly(3,4-ethylenedioxythiophene). Many researchers have focused on modifying PEDOT:PSS system with additives to enhance performance.[48–50] Some additives are usually added to improve the performance of PEDOT:PSS film including (i) EG, to enhance conductivity, (ii) dodecyl benzene sulfonic acid (DBSA), to adjust film-forming properties, and (iii) (3-glycidyloxypropyl) trimethoxysilane (GOPS), to crosslink the film for stable operation in aqueous conditions.[49] PEDOT:PSS-based OECTs that operate in depletion mode exhibit high g_m in the range of millisiemens and a response time in the range of tens of microsecond.[48] By solvent-assisted crystallization, crystallized PEDOT:PSS (Crys-P) exhibited remarkable OECT performance, with μC^* of 490 F cm^{-1} V^{-1} s^{-1}.[51] Poly(3,4-ethylenedioxythiophene) doped with tosylate (PEDOT:TOs) (Figure 5A) has a similar doping principle to PEDOT:PSS while tosylate (Tos) is a small molecule. By vapor-phase polymerization, a film cast from a precursor solution containing Tos moieties is exposed to EDOT vapor to yield the conducting polymer PEDOT:Tos.[52] By this process, researchers can also incorporate different biomolecules with PEDOT:Tos in the channel of OECTs, which makes the PEDOT:Tos a promising biological function material.[31]

ProDOT(OE)-DMP is an oligo(ether)-functionalized propylenedioxythiophene (ProDOT) copolymer (Figure 5A).[41] ProDOT(OE) was copolymerized using direct(hetero)arylation polymerization (DHAP) with 2,2-dimethyl (DMP) functionalized dibromo ProDOT, yielding ProDOT(OE)-DMP. Two OE side chains confer sufficient polarity for organic solubility and aqueous redox activity without rendering the polymer water-soluble. The DMP functionalized ProDOT ensures a low oxidation potential (low V_{th}) and enhances capacitance. Moreover, comparing to Stille cross-coupling, which is widely used for synthetic OECT polymers, DHAP, is more environmentally and biologically friendly. The OECTs based on ProDOT(OE)-DMP exhibit impressive performance and the design strategies can be used to develop more electrochemical active materials.

In terms of the second-generation semiconducting polymers for OECTs, making the best of side chain engineering is the main way to obtain high-performance OECT materials, including ionic chains, EG side chains, and alkyl spacers. Backbone engineering, such as BDT and XDOT, also brings lots of possibilities for the design of materials. Beyond that, the copolymerization of structural units with different functions is also a promising strategy via morphology control. Nevertheless, limited

performance modulation of the thiophene system and the lack of high-performance n-type materials are still the choke points for the development of OECT-based logic systems and sensors with amplification capability.[53] So more ingenious molecular design strategies are still needed.

3.2 | The third-generation semiconducting polymers for OECTs

The third-generation semiconducting polymers mainly refer to D–A polymers, which have huge energy level adjustability and high-carrier mobility compared to polythiophene. In the past few years, the fruitful chemical structures, readily modulated energy level, high-charge carrier mobilities have made D–A conjugated polymers very attractive in organic electronics.[54–58] Some of these building blocks have been introduced into the design of OECT polymers. Similar to polythiophene polymers, it is also particularly important to modify them to meet the ionic infiltration characteristics. Due to the better rigidity and planarity of the backbone, D–A polymers always suffer from poor solubility, which needs to be adjusted by side chains. Recently, many studies have focused on side chain engineering, which modulates the type, length, branching, and density of side chains to gain high-performance OECTs based on D–A polymers. In this part, we will summarize high-performance D–A polymers and special type polymers for OECTs and highlight their molecular design.

The p-type D–A polymers are studied extensively to catch up with and exceed the high performance of the second-generation semiconductors. At first, the performances of D–A polymers were poor and disappointing, but with further study in the past 10 years, the potential of p-type D–A polymers for OECTs is unleashed and their performances gradually approach most of the polythiophene derivatives (Table 1), as we will discuss below.

Inspired by CPE, Nguyen and co-workers utilized PCPDTBT-SO3K (CPE-K) as an active material of OECTs[59] (Figure 6A). CPE-K contains cyclopentadithiophene (CPDT) and benzothiadiazole (BT) alternating D–A units and is highly conductive because it is self-doped by the sulfonate side chains. CPE-K has been successfully used as a neutral interlayer in OPVs and as an active layer in thermoelectric devices, and also shows good performance in OECTs. Although this is the only study on D–A CPE so far, this molecular design may have great potential in the future.

Isoindigo (IID) is a well-established electron-deficient building block for D–A copolymers for solar cells and FETs.[60–62] Due to its two lactam rings, IID has a strong electron-withdrawing character and can shift energy level to a low LUMO. Yue and co-workers developed a series of IID-based polymers for OECTs. They mainly investigated the effect of EG and alkyl chains on the OECT performance. They used different side-chain functionalized IID units as donor and EDOT groups as acceptor to synthesis a series of p-type organic semiconducting polymers for OECTs, named PIBET.[63] Four different types of side chains are linked on the lactam nitrogen positions of IID: hybrid alkyl-EG chains (PIBET-AO), linear hydrophilic EG chains (PIBET-O), branched hydrophilic EG chains (PIBET-BO), and branched hydrophobic alkyl chains (PIBET-A) (Figure 6B). They also chose the bisthiophene unit as a comparison (PIBT-BO) (Figure 6C). PIBET-BO exhibited a much lower V_{th} than PIBT-BO. In addition, to affect characteristic parameters, side chains largely impact the operational stability of D-A polymers as well. OECTs based on PIBET-A showed the lowest $g_{m,norm,}$ and response speed due to the inefficient injection/ejection of hydrated electrolyte ions. Increasing the number of EG side chains from linear in PIBET-O to branched in PIBET-BO induced a decrease in $g_{m,norm}$ as well as device stability. PIBET-AO-based devices have a similar $g_{m,norm}$ with PIBET-O, while operational stability and substrate adhesion are drastically enhanced. Devices based on PIBET-AO exhibited preserved performance after extensive ultrasonication (1.5 h) or after continuous on–off switching for over 6 h, while the PIBET-A and PIBET-O based devices retain only 27 and 10% of the on currents after 40 minutes of on–off switching. The superior stability of PIBET-AO is ascribed to its alkyl fragments close to the backbone, which prevents alterations in film morphology and might negatively impact interchain transport and device performances over time. Therefore, a balanced combination of hydrophobic and hydrophilic chains is a potential way to develop long-term stable OECT semiconducting materials.

Diketopyrrolopyrrole (DPP) is one of the most extensively studied building blocks for building D–A polymers.[64] Giovannitti and co-workers synthesized copolymers based on pyridine-flanked DPP (PyDPP) with T2 or MeOT2, named p(gPyDPP-T2) and p(gPyDPP-2MeOT) (Figure 6D).[65] Due to the more localized wavefunction for the hole polaron which is expected to stabilize the hole polaron further, p(gPyDPP-2MeOT) exhibited better redox stability, just like gBDT-MeOT2.[47] Contrary to what we mentioned above, Giovannitti and co-workers emphasized that polymers with large IPs can shift the operational voltages of OECTs to avoid oxygen reduction reaction (ORR) occurring in ambient conditions. They demonstrated that p(gPyDPP-2MeOT) (IP = 5.0 eV) did not undergo ORR in ambient

TABLE 1 Summary of OECT performances for the polymers

Polymer	Generation	Type	V_{th}[a] (V)	$I_{on/off}$[a]	μC^*[b] ($Fcm^{-1} V^{-1} s^{-1}$)	μ[b] ($cm^2V^{-1} s^{-1}$)	C^* (Fcm^{-3})	τ_{on},τ_{off} (ms)	Reference[c]
P3MEEMT	2nd	p	−0.6	—	49	0.28	175	—	20
PTHS	2nd	p	−0.4	700	5.5	0.044	124	0.4	24,35
$PTHS^-TMA^+$-grad-P3HT	2nd	p	−0.15	10^5	1.7	0.017	100	—	26
PEDOT:PSS	2nd	p	0.4	10^5	47	1.2	39	0.1	24,49
Crys-P	2nd	p	—	—	490	4.34	113	—	51
ProDOT(OE)-DMP	2nd	p	−0.45	10^5	6.99	0.063	111	—	41
g2T-T	2nd	p	−0.2	1.7×10^5	167	0.76	220	1.4	23,24
P(g2T2-g4T2)	2nd	p	0.02	10^5	522	2.79	187	—	46
p(g2T-TT)	2nd	p	−0.2	10^5	261	1.08	241	0.42, 0.043	19,24
PIBET-AO	3rd	p	−0.44	2×10^4	—	—	—	590, 390	63
p(gPyDPP-MeOT2)	3rd	p	−0.35	10^5	1.8	0.03	60	0.77, 0.46	65
P(gDPP-T2)	3rd	p	−0.52	10^5	342	1.74	196	—	36
P(bgDPP-MeOT2)	3rd	p	−0.33	1.7×10^5	195	1.63	120	0.516, 0.03	39
PTDPP-DT	3rd	p	−0.93	10^5	149	—	—	—	67
BBL	3rd	n	0.35	6×10^3	0.65	0.0007	930	900, 200	71
p(gNDI-gT2)	3rd	n	0.35	3×10^3	0.18	0.00045	397	—	24,37
NDI-T2 (P-90)	3rd	n	0.25	3.6×10^3	0.047	0.000238	198	—	68
P(C6-T2)	3rd	n	0.3	—	1.29	0.00474	272	—	70
PgNaN	3rd	n	0.37	10^4	0.662	0.00662	100	—	38

Abbreviations: BBL, poly(benzimidazobenzophenanthroline); DMP, 2,2-dimethyl; PEDOT:PSS, poly(3,4-ethylenedioxythiophene) doped with poly(styrene sulfonate); ProDOT, propylenedioxythiophene; PTHS, poly(6[thiophene-3-yl]hexane-1-sulfonate) tetrabutylammonium; P3HT, Poly(3-hexylthiophene).

[a]The device sizes may vary from the article, and the electrolyte is 0.1 M NaCl aqueous solution.

[b]μC^* and μ are the average data calculated from g_m.

[c]The parameter sources of μC^*, μ, C^*, τ may be different from others

— means the data are missing in the literature.

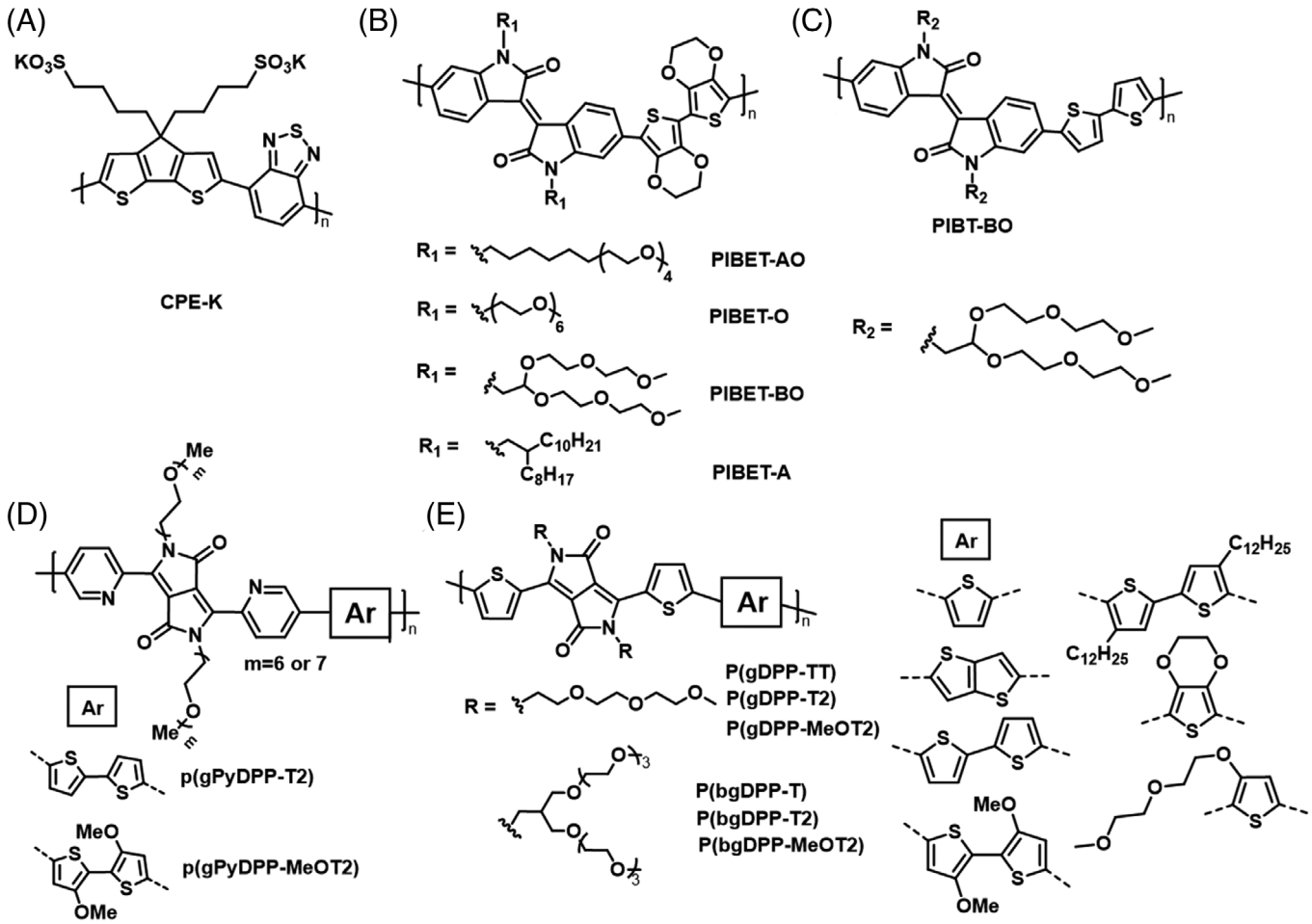

FIGURE 6 Chemical structures of the p-type third-generation semiconducting polymers for OECTs. (A) CPE-K.[59] (B and C) IID-based polymers.[63] (D) PyDPP-based polymers.[65] (E) DPP-based polymers.[36,39,66,67] DPP, diketopyrrolopyrrolep; IID, Isoindigo; OECTs, organic electrochemical transistors; PyDPP, pyridine-flanked DPP

conditions, while PEDOT:PSS and p(g2T-TT) (Figures 5A and 4F) were observed spontaneous ORR. Furthermore, both PEDOT:PSS and p(g2T-TT) predominantly produced H_2O_2, which does harm to local biological environment and may accelerate device degradation while p(gPyDPP-MeOT2) would form mostly H_2O during ORR. The molecular design strategy presented in the achievement is viable for developing bioelectronic materials with no hazardous side-products and low-power consumption.

In the past 2 years, as a versatile building block, D–A polymers based on DPP in OECTs have been studied extensively. McCulloch et al.[36] and Lei et al.[39] reported DPP-based high-performance OECTs separately almost at the same time (Figure 6E). Although the backbone structure is the same, they get different results and conclusions. McCulloch and co-workers found p(gDPP-T2) showed the highest μC^* and p(gDPP-MeOT2) had the lowest performance of 57 F cm^{-1} V^{-1} s^{-1}, which is attributed to different polaron delocalization by authors. However, with the same backbone structure and longer/branched side-chain, Lei and co-workers found the strongest electron-donating moiety MeOT2 was the best donor, and the performance can be optimized to 216 F cm^{-1} V^{-1} s^{-1}. Moreover, they summarized a series of strategies for high-performance OECTs, including donor, side chain, molecular weight, and processing conditions. Strong electron-donating moiety, branched EG chains, optimized polymerization conditions and polar solvent are the keys to get high-performance D–A polymers for OECT. These results have revealed the complexity and systematization of D–A polymers with EG side chains. In addition, other DPP-based polymers with different donors and side chains are studied.[66,67]

Because it is difficult to lower the LUMO energy levels to achieve electron transport and maintain air stability, high-performance n-type conjugated polymers are very rare. Moreover, the existence of electrolyte (most commonly NaCl solution) aggravates the instability of polymers and makes the development of n-type OECTs

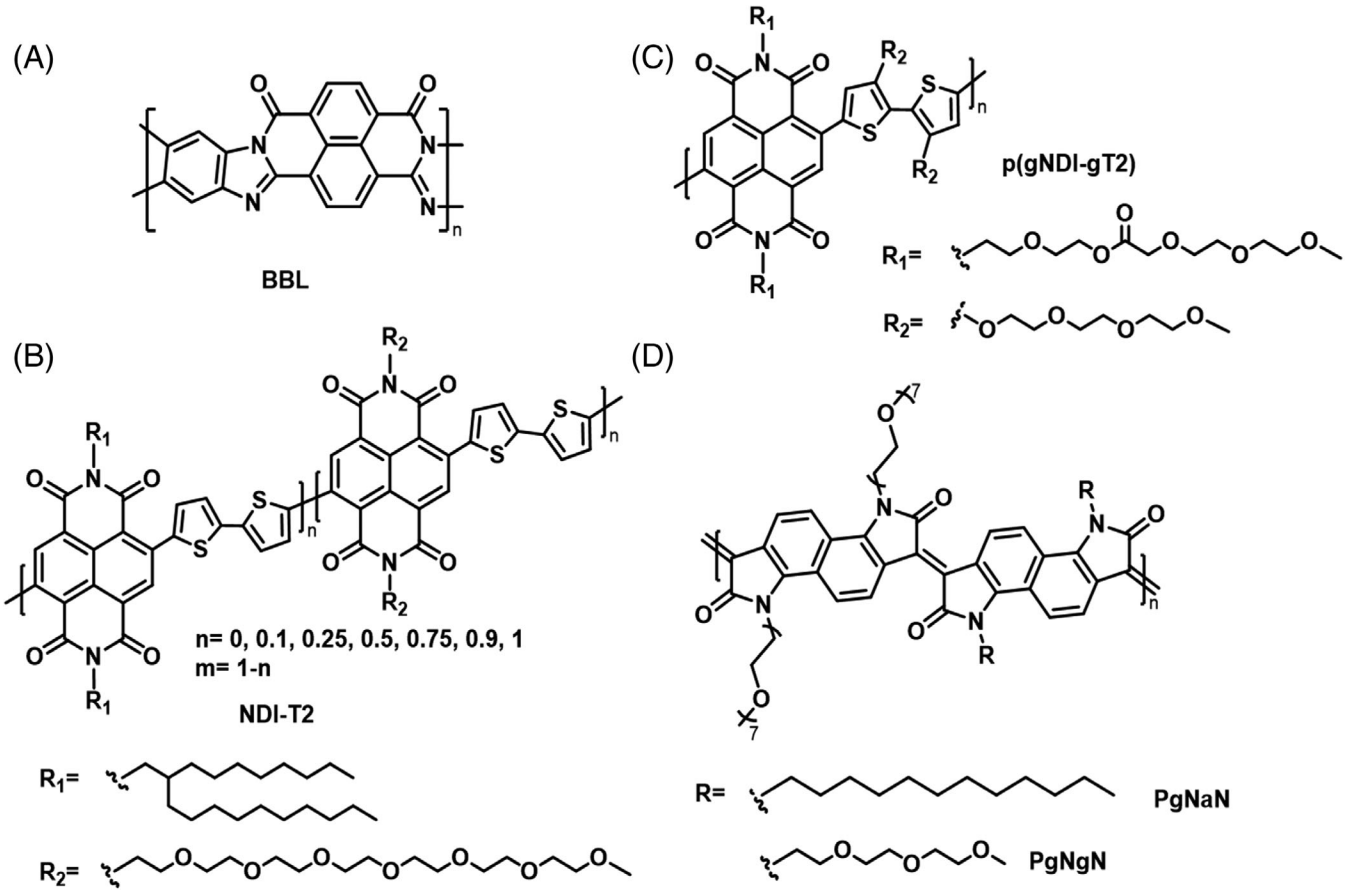

FIGURE 7 Chemical structures of some n-type semiconducting polymers for OECTs, (A) BBL.[71] (B) p(gNDI-gT2).[37] (C) NDI-T2,[68] from P-0 to P-100, including P-90. (D) PgNaN and PgNgN.[38] BBL, poly(benzimidazobenzophenanthroline); NDI-T2, naphthalene-1,4,5,8-tetracarboxylic-diimide-bithiophene; OECTs, organic electrochemical transistors

troublesome. The lack of n-type polymers whose performances can be comparable to p-type restricts the development of complementary logic circuits, which are the basis of flexible electronics. D–A polymers and special-type polymers, including donor–donor polymers and ladder-type polymers, enable the implementation of n-type OECTs.

The first n-type OECT polymer is a napthalenediimide-bithiophene polymer (p[gNDI-gT2]) (Figure 7B) developed by Giovannitti and co-workers.[37] NDI is a highly electron-deficient unit while bithiophene is electron-rich. The backbone structure contributes to a high electron affinity (EA = 4.12 eV), and a low ionization potential (IP = 4.83 eV) of the polymer. The ambipolar OECTs based on p(gNDI-gT2) exhibited relatively balanced ambipolar charge transport characteristics and showed no degradation under 2 hours continuous cycling in water at proper operating voltage. This achievement demonstrates that water-stable n-type polymers are achievable and indicates a new direction for n-type conjugated polymers. In a follow-up study, Giovannitti and co-workers developed a series of D–A polymers based on naphthalene-1,4,5,8-tetracarboxylic-diimide-bithiophene (NDI-T2) (Figure 7C) to study how the substitution of alkyl side chain with EG side chains affects device performances.[68] These random copolymers are named P-0 to P-100 with the increasing percentage of the EG chain. To achieve stable volumetric charging (pure OECT mode), the EG chain needs to be at least 50% (P-50), while polymers with lower EG chain percentages showed a mixed operation and required high-operation voltages. Among the polymers, P-90 exhibited the most outstanding OECT characteristic (μ, C^*, $g_{m,norm}$). The reduction voltage onset (V_{th}) decreased from 1.1 to 0.2 V with the percentage increasing from 0 to 100%. NDI-T2 copolymers with alkyl chains show high-electron mobilities ($\mu_{P\text{-}0} = 0.132\ cm^2\ V^{-1}\ s^{-1}$), while the electron mobility drops rapidly when the alkyl chains are replaced by polar EG chains ($\mu_{P\text{-}25} = 0.00184\ cm^2\ V^{-1}\ s^{-1}$, $\mu_{P\text{-}90} = 0.000238\ cm^2\ V^{-1}\ s^{-1}$). This achievement alerts us to the merits and shortcomings of EG chains, which we should take into account in studies and applications. How to obtain high C^* while preventing the attenuation of mobility is still a hard nut to crack. Recently, the modulation of alkyl spacers and side chains has been explored on

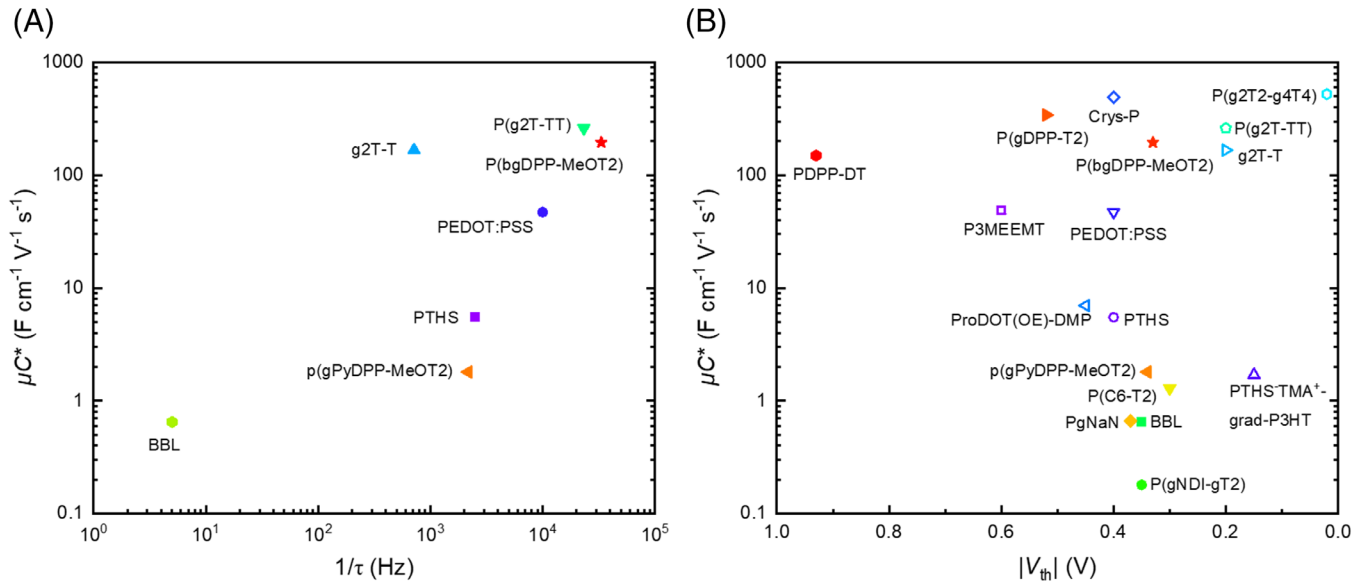

FIGURE 8 Summary of OECT performances via (A) μC^*-$1/\tau$, and (B) μC^*-$|V_{th}|$ plot for the polymers in Table 1. The polymers in the upper right corner of both images have better overall properties. The response speed is limited to 1–10^5 Hz for OECTs and shows a large variation among polymers. Although the μC^* value of many polymers is outstanding, the $|V_{th}|$ of the device is unsatisfactory, which is more obvious in D–A polymers. OECT, organic electrochemical transistor

NDI-T2,[69,70] and the highest μC^* for n-type can be optimized to 1.29 F cm^{-1} V^{-1} s^{-1} (P[C6-T2]).

Among the third-generation semiconducting polymers for OECTs, the most unique n-type polymer is poly (benzimidazobenzophenanthroline) (BBL)[71] (Figure 7A). BBL is a ladder-type polymer with high rigidity and planarity of the π-conjugated polymer backbone, leading to high EA. The backbone and no side chain characteristic promote delocalization of the carriers in BBL and make intramolecular transfer easier, thus providing high-polaron mobility along the ladder-type chain. The structure advantages lead to the high C^* of BBL, and OECTs based on BBL show high transconductance and excellent stability in ambient and aqueous media (1 h switching test).

Recently, McCulloch and co-workers developed high-performance n-type polymers[38] (Figure 7D). With only electron-deficient units and a torsion-free backbone, the PgNaN and PgNgN have deep-lying LUMO lower than −4.0 eV. The alkyl chain of PgNaN improved the solubility during polymerization and helped gain larger molecular weight than PgNgN. The PgNaN shows high-OECTs performance with an average μC^* of 0.662 F cm^{-1} V^{-1} s^{-1}, and the metal-free aldol condensation polymerization is a benefit for the application of bioelectronics.

Up to now, these D–A polymers have shown huge potential in OECTs, especially for n-type devices, and performances of p-type polymers gradually approaching the polythiophene system. We believe that with the in-depth study of the charge transport mechanism in OECTs and the further expansion of material structures, D–A polymers will show superior performances and exert their advantages in researches and applications.

4 | CONCLUSIONS AND OUTLOOK

The past decade has witnessed the prosperity and fast development of OECTs. Effective molecular design strategies, various device structures, and several promising applications have been explored. In this article, we particularly emphasize the role of molecular design strategies toward high-performance OECTs. As discussed above, we could conclude that: (i) proper hydrophilic side chains, such as EG chains, ionic chains, alkyl spacers, and partially alkyl/EG chains can ensure adequate ion infiltration during the electrochemical doping/dedoping process while minimizing unwelcome side effect to hole/electron transport; (ii) backbone engineering can adjust frontier orbital energy levels, intermolecular interactions, and thereby charge carrier mobilities, and so on.; (iii) the interaction between the side chains and the backbone may influence molecular packing, device stability, and other parameters (e.g., response time).

Multiple processes are involved in the operation of OECTs, including ion injection, redox charging, and electron transport. However, a clear structure–property relationship has not been well established. For instance,

there may be a trade-off between μ and C^* in OECTs, and thus the optimum side chain type, length, and distribution may vary from polymer to polymer. Besides, D–A polymers have exhibited superior performances in OFETs, OPVs, and other organic electronics, while in OECTs, the performance of the polythiophene system is still better than those of D–A polymers (Table 1). For these issues, we conjecture and have partially proven that different polymerization methods, processing conditions, the batch-to-batch variation (especially for molecular weight) will all influence device performances, which cannot be ascribed only to poor molecular design issues.[39] Besides, many other factors, including molecular packing,[72] supramolecular assembly,[73] film morphology,[74] and counterions[75,76] also have great influences on device performance, which have not been fully explored and understood yet. Therefore, careful molecular design is just the first step for the performance enhancement, and during the study of materials, we need to consider all the influential factors more comprehensively.

In addition, the evaluation methods for an OECT device still need to be improved and unified. In terms of device stability, there are various evaluation methods, including long-time switching test, adhesion ability to substrate, ORR, and so on. Whether the description of stability should be subdivided into several parameters or unified as a specific parameter needs to be considered. Furthermore, many parameters of OECTs are directly related to the device size, including g_m and τ, which makes them hard to compare among different materials. We imagine that it would be much beneficial if we could compare certain parameters with unified device configuration.

As a growing field, there are still many challenges that have not been addressed in OECTs. N-type materials are still in shortage and their performances lag far behind that of the p-type ones, which impedes the development of OECT-based amplifiers and logic circuits. Besides, slow response time (τ) is one of the major drawbacks for OECTs (Figure 8A). The development of real-time sensing and high-speed devices requires further reduction of τ, while, as we know, no effective material design method has been developed for reducing the response time yet. Moreover, the fabrication of OECTs is still on a small scale. Even so, we have observed a large variation among different devices. Thus, how to achieve satisfactory performance with good uniformity at large-scare is also an important issue.[77] Last but not least, the V_{th} is an often ignored parameter compared to μC^*. Theoretically, the $|V_g|$ should be less than 0.6 V (vs. Ag/AgCl) to avoid harmful side reactions in aqueous solutions,[19] and low V_{th} can lower the operating voltage of devices to realize low-power consumption and long operation life. As shown in Figure 8B, many high-μC^* materials have shown large $|V_{th}|$, especially for D–A polymers. Therefore, reducing the threshold voltage to gain maximum transconductance at nearly zero gate bias is desirable for many biosensing applications.

ACKNOWLEDGMENTS

This work is supported by the National Natural Science Foundation of China (22075001), and the Open Fund of the State Key Laboratory of Luminescent Materials and Devices (South China University of Technology, 2021-skllmd-02).

DATA AVAILABILITY STATEMENT

Data sharing is not applicable to this paper as no new data were created or analyzed in this review.

ORCID

Peiyun Li https://orcid.org/0000-0001-7805-527X
Ting Lei https://orcid.org/0000-0001-8190-9483

REFERENCES

[1] H. S. White, G. P. Kittlesen, M. S. Wrighton, *J. Am. Chem. Soc.* **1984**, *106*, 5375.
[2] G. P. Kittlesen, H. S. White, M. S. Wrighton, *J. Am. Chem. Soc.* **1984**, *106*, 7389.
[3] B. D. Paulsen, K. Tybrandt, E. Stavrinidou, J. Rivnay, *Nat. Mater.* **2020**, *19*, 13.
[4] S. Chen, A. Surendran, X. Wu, S. Y. Lee, M. Stephen, W. L. Leong, *Adv. Mater. Technol.* **2020**, *5*, 2000523.
[5] M. Sessolo, J. Rivnay, E. Bandiello, G. G. Malliaras, H. J. Bolink, *Adv. Mater.* **2014**, *26*, 4803.
[6] S. Wustoni, C. Combe, D. Ohayon, M. H. Akhtar, I. McCulloch, S. Inal, *Adv. Funct. Mater.* **2019**, *29*, 1904403.
[7] O. Parlak, S. T. Keene, A. Marais, V. F. Curto, A. Salleo, *Sci. Adv.* **2018**, *4*, eaar2904.
[8] J. T. Reeder, J. Choi, Y. Xue, P. Gutruf, J. Hanson, M. Liu, T. Ray, A. J. Bandodkar, R. Avila, W. Xia, S. Krishnan, S. Xu, K. Barnes, M. Pahnke, R. Ghaffari, Y. Huang, J. A. Rogers, *Sci. Adv.* **2019**, *5*, eaau6356.
[9] X. Yang, T. Zhou, T. J. Zwang, G. Hong, Y. Zhao, R. D. Viveros, T. M. Fu, T. Gao, C. M. Lieber, *Nat. Mater.* **2019**, *18*, 510.
[10] Y. Liu, A. F. McGuire, H. Y. Lou, T. L. Li, J. B. Tok, B. Cui, Z. Bao, *Proc. Natl. Acad. Sci. U. S. A.* **2018**, *115*, 11718.
[11] P. Gkoupidenis, N. Schaefer, B. Garlan, G. G. Malliaras, *Adv. Mater.* **2015**, *27*, 7176.
[12] B. Winther-Jensen, B. Kolodziejczyk, O. Winther-Jensen, *APL Mater.* **2015**, *3*, 014903.
[13] C. Qian, J. Sun, L. A. Kong, G. Gou, J. Yang, J. He, Y. Gao, Q. Wan, *ACS Appl. Mater. Interfaces* **2016**, *8*, 26169.
[14] S. T. Keene, A. Melianas, E. J. Fuller, Y. van de Burgt, A. A. Talin, A. Salleo, *J. Phys. D: Appl. Phys.* **2018**, *51*, 224002.
[15] M. Moser, J. F. Ponder, A. Wadsworth, A. Giovannitti, I. McCulloch, *Adv. Funct. Mater.* **2018**, *29*, 1807033.

[16] H. Shi, C. Liu, Q. Jiang, J. Xu, *Adv. Electron. Mater.* **2015**, *1*, 1500017.
[17] A. J. Heeger, *Chem. Soc. Rev.* **2010**, *39*, 2354.
[18] A. Laiho, L. Herlogsson, R. Forchheimer, X. Crispin, M. Berggren, *Proc. Natl. Acad. Sci. U. S. A.* **2011**, *108*, 15069.
[19] A. Giovannitti, D. T. Sbircea, S. Inal, C. B. Nielsen, E. Bandiello, D. A. Hanifi, M. Sessolo, G. G. Malliaras, I. McCulloch, J. Rivnay, *Proc. Natl. Acad. Sci. U. S. A.* **2016**, *113*, 12017.
[20] L. Q. Flagg, C. G. Bischak, J. W. Onorato, R. B. Rashid, C. K. Luscombe, D. S. Ginger, *J. Am. Chem. Soc.* **2019**, *141*, 4345.
[21] R. Giridharagopal, L. Q. Flagg, J. S. Harrison, M. E. Ziffer, J. Onorato, C. K. Luscombe, D. S. Ginger, *Nat. Mater.* **2017**, *16*, 737.
[22] D. A. Bernards, G. G. Malliaras, *Adv. Funct. Mater.* **2007**, *17*, 3538.
[23] C. B. Nielsen, A. Giovannitti, D. T. Sbircea, E. Bandiello, M. R. Niazi, D. A. Hanifi, M. Sessolo, A. Amassian, G. G. Malliaras, J. Rivnay, I. McCulloch, *J. Am. Chem. Soc.* **2016**, *138*, 10252.
[24] S. Inal, G. G. Malliaras, J. Rivnay, *Nat. Commun.* **2017**, *8*, 1767.
[25] D. Rawlings, E. M. Thomas, R. A. Segalman, M. L. Chabinyc, *Chem. Mater.* **2019**, *31*, 8820.
[26] P. Schmode, D. Ohayon, P. M. Reichstein, A. Savva, S. Inal, M. Thelakkat, *Chem. Mater.* **2019**, *31*, 5286.
[27] V. Kaphle, P. R. Paudel, D. Dahal, R. K. Radha Krishnan, B. Lussem, *Nat. Commun.* **2020**, *11*, 2515.
[28] D. Y. Tu, S. Fabiano, *Appl. Phys. Lett.* **2020**, *117*, 080501.
[29] J. Nissa, P. Janson, M. Berggren, D. T. Simon, *Adv. Electron. Mater.* **2021**, *7*, 2001173.
[30] R. Colucci, H. F. D. Barbosa, F. Gunther, P. Cavassin, G. C. Faria, *Flex. Print. Electron.* **2020**, *5*, 013001.
[31] J. Rivnay, S. Inal, A. Salleo, R. M. Owens, M. Berggren, G. G. Malliaras, *Nat. Rev. Mater.* **2018**, *3*, 17086.
[32] R. Noriega, J. Rivnay, K. Vandewal, F. P. Koch, N. Stingelin, P. Smith, M. F. Toney, A. Salleo, *Nat. Mater.* **2013**, *12*, 1038.
[33] Z. S. Parr, R. B. Rashid, B. D. Paulsen, B. Poggi, E. Tan, M. Freeley, M. Palma, I. Abrahams, J. Rivnay, C. B. Nielsen, *Adv. Electron. Mater.* **2020**, *6*, 2000215.
[34] C. G. Bischak, L. Q. Flagg, K. Yan, C. Z. Li, D. S. Ginger, *ACS Appl. Mater. Interfaces* **2019**, *11*, 28138.
[35] S. Inal, J. Rivnay, P. Leleux, M. Ferro, M. Ramuz, J. C. Brendel, M. M. Schmidt, M. Thelakkat, G. G. Malliaras, *Adv. Mater.* **2014**, *26*, 7450.
[36] M. Moser, A. Savva, K. Thorley, B. D. Paulsen, T. C. Hidalgo, D. Ohayon, H. Chen, A. Giovannitti, A. Marks, N. Gasparini, A. Wadsworth, J. Rivnay, S. Inal, I. McCulloch, *Angew. Chem., Int. Ed.* **2020**, *60*, 7777.
[37] A. Giovannitti, C. B. Nielsen, D. T. Sbircea, S. Inal, M. Donahue, M. R. Niazi, D. A. Hanifi, A. Amassian, G. G. Malliaras, J. Rivnay, I. McCulloch, *Nat. Commun.* **2016**, *7*, 13066.
[38] X. Chen, A. Marks, B. D. Paulsen, R. Wu, R. B. Rashid, H. Chen, M. Alsufyani, J. Rivnay, I. McCulloch, *Angew. Chem., Int. Ed.* **2021**, *60*, 9368.
[39] H. Jia, Z. Huang, P. Li, S. Zhang, Y. Wang, J.-Y. Wang, X. Gu, T. Lei, *J. Mater. Chem. C* **2021**, *9*, 4927.
[40] L. Giraud, S. Grelier, E. Grau, G. Hadziioannou, C. Brochon, H. Cramail, E. Cloutet, *J. Mater. Chem. C* **2020**, *8*, 9792.
[41] L. R. Savagian, A. M. Osterholm, J. F. Jr Ponder, K. J. Barth, J. Rivnay, J. R. Reynolds, *Adv. Mater.* **2018**, *30*, e1804647.
[42] P. Schmode, A. Savva, R. Kahl, D. Ohayon, F. Meichsner, O. Dolynchuk, T. Thurn-Albrecht, S. Inal, M. Thelakkat, *ACS Appl. Mater. Interfaces* **2020**, *12*, 13029.
[43] E. Zeglio, O. Inganas, *Adv. Mater.* **2018**, *30*, e1800941.
[44] A. Savva, R. Hallani, C. Cendra, J. Surgailis, T. C. Hidalgo, S. Wustoni, R. Sheelamanthula, X. Chen, M. Kirkus, A. Giovannitti, A. Salleo, I. McCulloch, S. Inal, *Adv. Funct. Mater.* **2020**, *30*, 1907657.
[45] M. Moser, L. R. Savagian, A. Savva, M. Matta, J. F. Ponder, T. C. Hidalgo, D. Ohayon, R. Hallani, M. Reisjalali, A. Troisi, A. Wadsworth, J. R. Reynolds, S. Inal, I. McCulloch, *Chem. Mater.* **2020**, *32*, 6618.
[46] M. Moser, T. C. Hidalgo, J. Surgailis, J. Gladisch, S. Ghosh, R. Sheelamanthula, Q. Thiburce, A. Giovannitti, A. Salleo, N. Gasparini, A. Wadsworth, I. Zozoulenko, M. Berggren, E. Stavrinidou, S. Inal, I. McCulloch, *Adv. Mater.* **2020**, *32*, e2002748.
[47] A. Giovannitti, K. J. Thorley, C. B. Nielsen, J. Li, M. J. Donahue, G. G. Malliaras, J. Rivnay, I. McCulloch, *Adv. Funct. Mater.* **2018**, *28*, 1706325.
[48] D. Khodagholy, J. Rivnay, M. Sessolo, M. Gurfinkel, P. Leleux, L. H. Jimison, E. Stavrinidou, T. Herve, S. Sanaur, R. M. Owens, G. G. Malliaras, *Nat. Commun.* **2013**, *4*, 2133.
[49] J. Rivnay, P. Leleux, M. Sessolo, D. Khodagholy, T. Herve, M. Fiocchi, G. G. Malliaras, *Adv. Mater.* **2013**, *25*, 7010.
[50] X. Wu, A. Surendran, J. Ko, O. Filonik, E. M. Herzig, P. Muller-Buschbaum, W. L. Leong, *Adv. Mater.* **2019**, *31*, e1805544.
[51] S. M. Kim, C. H. Kim, Y. Kim, N. Kim, W. J. Lee, E. H. Lee, D. Kim, S. Park, K. Lee, J. Rivnay, M. H. Yoon, *Nat. Commun.* **2018**, *9*, 3858.
[52] B. Winther-Jensen, K. West, *Macromolecules* **2004**, *37*, 4538.
[53] P. Romele, P. Gkoupidenis, D. A. Koutsouras, K. Lieberth, Z. M. Kovacs-Vajna, P. W. M. Blom, F. Torricelli, *Nat. Commun.* **2020**, *11*, 3743.
[54] J. Mei, Y. Diao, A. L. Appleton, L. Fang, Z. Bao, *J. Am. Chem. Soc.* **2013**, *135*, 6724.
[55] T. Lei, J. Y. Wang, J. Pei, *Acc. Chem. Res.* **2014**, *47*, 1117.
[56] B. Sun, W. Hong, Z. Yan, H. Aziz, Y. Li, *Adv. Mater.* **2014**, *26*, 2636.
[57] H. N. Tsao, D. M. Cho, I. Park, M. R. Hansen, A. Mavrinskiy, D. Y. Yoon, R. Graf, W. Pisula, H. W. Spiess, K. Mullen, *J. Am. Chem. Soc.* **2011**, *133*, 2605.
[58] X. Yan, M. Xiong, J. T. Li, S. Zhang, Z. Ahmad, Y. Lu, Z. Y. Wang, Z. F. Yao, J. Y. Wang, X. Gu, T. Lei, *J. Am. Chem. Soc.* **2019**, *141*, 20215.
[59] A. T. Lill, D. X. Cao, M. Schrock, J. Vollbrecht, J. Huang, T. Nguyen-Dang, V. V. Brus, B. Yurash, D. Leifert, G. C. Bazan, T. Q. Nguyen, *Adv. Mater.* **2020**, *32*, e1908120.
[60] E. Wang, W. Mammo, M. R. Andersson, *Adv. Mater.* **2014**, *26*, 1801.
[61] T. Lei, J. H. Dou, Z. J. Ma, C. H. Yao, C. J. Liu, J. Y. Wang, J. Pei, *J. Am. Chem. Soc.* **2012**, *134*, 20025.

[62] T. Lei, J. H. Dou, J. Pei, *Adv. Mater.* **2012**, *24*, 6457.
[63] Y. Wang, E. Zeglio, H. Liao, J. Xu, F. Liu, Z. Li, I. P. Maria, D. Mawad, A. Herland, I. McCulloch, W. Yue, *Chem. Mater.* **2019**, *31*, 9797.
[64] Y. Sui, Y. Deng, T. Du, Y. Shi, Y. Geng, *Mater. Chem. Front.* **2019**, *3*, 1932.
[65] A. Giovannitti, R. B. Rashid, Q. Thiburce, B. D. Paulsen, C. Cendra, K. Thorley, D. Moia, J. T. Mefford, D. Hanifi, D. Weiyuan, M. Moser, A. Salleo, J. Nelson, I. McCulloch, J. Rivnay, *Adv. Mater.* **2020**, *32*, e1908047.
[66] G. Krauss, F. Meichsner, A. Hochgesang, J. Mohanraj, S. Salehi, P. Schmode, M. Thelakkat, *Adv. Funct. Mater.* **2021**, *31*, 2010048.
[67] X. Wu, Q. Liu, A. Surendran, S. E. Bottle, P. Sonar, W. L. Leong, *Adv. Electron. Mater.* **2020**, *7*, 2000701.
[68] A. Giovannitti, I. P. Maria, D. Hanifi, M. J. Donahue, D. Bryant, K. J. Barth, B. E. Makdah, A. Savva, D. Moia, M. Zetek, P. R. F. Barnes, O. G. Reid, S. Inal, G. Rumbles, G. G. Malliaras, J. Nelson, J. Rivnay, I. McCulloch, *Chem. Mater.* **2018**, *30*, 2945.
[69] I. P. Maria, B. D. Paulsen, A. Savva, D. Ohayon, R. Wu, R. Hallani, A. Basu, W. Du, T. D. Anthopoulos, S. Inal, J. Rivnay, I. McCulloch, A. Giovannitti, *Adv. Funct. Mater.* **2021**, *31*, 2008718.
[70] D. Ohayon, A. Savva, W. Du, B. D. Paulsen, I. Uguz, R. S. Ashraf, J. Rivnay, I. McCulloch, S. Inal, *ACS Appl. Mater. Interfaces* **2021**, *13*, 4253.
[71] H. Sun, M. Vagin, S. Wang, X. Crispin, R. Forchheimer, M. Berggren, S. Fabiano, *Adv. Mater.* **2018**, *30*, 1704916.
[72] C. G. Bischak, L. Q. Flagg, K. Yan, T. Rehman, D. W. Davies, R. J. Quezada, J. W. Onorato, C. K. Luscombe, Y. Diao, C. Z. Li, D. S. Ginger, *J. Am. Chem. Soc.* **2020**, *142*, 7434.
[73] C. Musumeci, M. Vagin, E. Zeglio, L. Ouyang, R. Gabrielsson, O. Inganäs, *J. Mater. Chem. C* **2019**, *7*, 2987.
[74] J. Surgailis, A. Savva, V. Druet, B. D. Paulsen, R. H. Wu, A. Hamidi-Sakr, D. Ohayon, G. Nikiforidis, X. X. Chen, I. McCulloch, J. Rivnay, S. Inal, *Adv. Funct. Mater.* **2021**, *31*, 2010165.
[75] C. G. Bischak, L. Q. Flagg, D. S. Ginger, *Adv. Mater.* **2020**, *32*, e2002610.
[76] C. Cendra, A. Giovannitti, A. Savva, V. Venkatraman, I. McCulloch, A. Salleo, S. Inal, J. Rivnay, *Adv. Funct. Mater.* **2019**, *29*, 1807034.
[77] J. Choi, R. Ghaffari, L. B. Baker, J. A. Rogers, *Sci. Adv.* **2018**, *4*, eaar3921.

AUTHOR BIOGRAPHIES

Peiyun Li obtained her BE in materials science from Huazhong University of Science and Technology in 2019. She is currently pursuing her PhD at Peking University. Her research focuses on organic electrochemical transistors and their applications in flexible electronics, neuromorphic computing, and bioelectronics.

Ting Lei is an Assistant Professor in the School of Materials Science & Engineering, Peking University. He received BS and PhD from Peking University in 2008 and 2013. After a postdoc training in Stanford, he joined Peking University in 2018. His current researches focus on organic/polymer functional materials, organic electronics, carbon-based electronics, and bioelectronics.

How to cite this article: P. Li, T. Lei, *J. Polym. Sci.* **2022**, *60*(3), 377. https://doi.org/10.1002/pol.20210503